

CT MEASUREMENT OF SAP VOIDS IN CONCRETE

**Sara Laustsen ⁽¹⁾, Dale P. Bentz ⁽²⁾, Marianne Tange Hasholt ⁽¹⁾ and
Ole Mejlhede Jensen ⁽¹⁾**

(1) Technical University of Denmark, Lyngby, Denmark

(2) National Institute of Standards and Technology, Gaithersburg, USA

Abstract

This paper describes how X-ray computed tomography (CT) scanning can be used to determine the void distribution in hardened concrete. Three different approaches are used to analyse a binary data set created from CT measurement. One approach classifies a cluster of connected, empty voxels (volumetric pixel of a 3D image) as one void, whereas the other two approaches are able to classify a cluster of connected, empty voxels as a number of individual voids. Superabsorbent polymers (SAP) have been used to incorporate air into concrete. An advantage of using SAP is that it enables control of the amount and size of the created air voids. The results indicate the presence of void clusters. To identify the individual voids, special computational approaches are needed. The addition of SAP results in a dominant peak in two of the three air void distributions. Based on the position (void diameter) of this peak, it is possible to calculate the liquid absorption of the SAP within the fresh concrete. This estimated liquid absorption is in agreement with measurements carried out in previous studies.

1. Introduction

A proper characterisation of air voids in hardened concrete should, in addition to the total air content, preferably provide knowledge about both the size distribution and geometric (spatial) distribution of air voids.

Characterisation of the air void system in hardened concrete is often carried out according to the linear-traverse method or the modified point-count method [1,2]. The linear-traverse method provides data about the measured traverse length through air voids and surrounding concrete, whereas the data obtained according to the modified point-count method are the number of points in air voids and in the surrounding concrete. The number of air voids intersected by the line of traverse is obtained with both methods.

Both methods are used to calculate the air content and the average size of air voids. Results from both methods may be influenced by sample preparation. Moreover, both methods have the weakness that they are based on 2D observations but have to describe 3D structures.

1.1 X-ray computed tomography scanning

X-ray computed tomography (CT) scanning is a powerful measuring technique which can provide information about the 3D structure of a sample without any preceding preparation [3], contrary to traditional methods for air void analyses. 2D and 3D images are generated based on a set of 2D X-ray images. The images in 2D and 3D can be used to investigate the internal structure of a specimen. The specimen is placed on a rotating table between an X-ray source and an X-ray detector. X-rays are sent through the specimen, for each position of the rotating table. This results in 2D X-ray transmission images of each slice. These images of the slices are reconstructed using special algorithms to produce a 3D data set for the specimen structure. A more detailed description of CT systems is given by Promentilla, Sugiyama and Shimura [4].

This paper describes three different approaches to determine the air void distribution in concrete based on data from CT scanning. Voids have been incorporated into concrete using superabsorbent polymers (SAP). The term “SAP void” is in this paper used for a SAP generated void, including the SAP particle. Compared with traditional air-entrainment, an advantage of using SAP is that it enables one to control the amount and the size of the created SAP voids.

2. Materials

Material data and composition of the investigated concrete are given in Table 1. The water-to-cement ratio (w/c) is 0.45. Extra water is added to account for water absorption by SAP particles, corresponding to an entrained w/c of 0.09 [5].

Table 1: Composition for 1 m³ of concrete. Aggregate densities refer to the saturated, surface dry state.

	Type	Size [mm]	Absorption [%]	Density [kg/m ³]	Mass [kg]	Volume [m ³]
Cement	CEM I 52.5 N	-	-	3160	494	0.156
Water	Tap water	-	-	1000	222 + 43*	0.222 + 0.043*
Sand	Sea sand	0-4	0.2	2640	754	0.286
Stone	Granite	4-8	0.6	2710	151	0.056
Stone	Granite	8-11	0.6	2720	604	0.222
Entrapped air (Estimate)	-	-	-	-	-	0.012
SAP (dry)	*	0.4*	1250*	1500*	4*	0.003*

* See text for explanation.

The SAP is a covalently crosslinked acrylamide/acrylic acid copolymer made by suspension polymerization. The SAP mainly consists of spherical particles that have been sieved into a size fraction of 150 μm to 160 μm in the dry state. Previous studies have indicated that their water absorption is approximately 12.5 gram water per gram dry SAP, which corresponds to 1250 % [5]. Based on this assumed value, the dry SAP absorbs 43 kg of water (per 1 m^3 of concrete) during mixing and creates voids in concrete with a size between 405 μm and 432 μm . The density of the swollen SAP particles is approximately 1025 kg/m^3 . The resulting SAP voids make up 4.6 % of the concrete volume.

3. Methods

Concrete was cast in a $\text{Ø}150 \times 300$ mm cylinder. The cylinder was demoulded one day after casting and stored in water for six days at approximately 20 °C. Subsequently, the cylinder was stored in a climate chamber for 15 days at approximately 20 °C and 65 % relative humidity. A 20 mm x 20 mm x 20 mm cube was cut from the centre of the cylinder after 22 days. A Y.CT Precision instrument from Yxlon International was used for CT scanning.¹

3.1 Analysis method

The obtained data set from CT scanning consists of 1114, 1090, and 1102 voxels in the x, y and z directions, respectively. The cubic voxel size (volumetric pixel of a 3D image) is approximately 20 μm . The centre xy plane of the data set is shown in Figure 1. A centred 500 voxel x 500 voxel x 500 voxel cube is extracted from the original data to reduce the influence of edge effects. The centre xy plane of the 500³ voxel cube is marked in Figure 1 and shown in Figure 2.

A 5x5x5 median filter is applied to the 500³ voxel cube to reduce noise [3]. Tests showed that a smaller filter window would not reduce noise satisfactorily. A median filter is a nonlinear filter which smoothes the image. An adequately smoothed image improves edge detection, which will assist in separating the air voids from the other phases in the concrete. The median filter is applied to the image voxel by voxel. Each voxel is surrounded by a volume of interest. For a 5x5x5 median filter the volume to be considered consists of 125 voxels with the studied voxel in the centre. The voxel values for the 125 voxels are sorted numerically beginning with the lowest value. The median value is assigned to the studied voxel. The centre xy plane of the filtered 500³ voxel cube is shown in Figure 3.

A threshold value was used to binarize the data set. The threshold value was determined based on a visual assessment of three xy planes (located at $z = 125, 250$ and 375). Three approaches, denoted as A, B1 and B2, were used to recognize voids in the binary data set. For each approach, it was possible to include and exclude volumes of connected, empty voxels at the edge. Each approach provides information about the volumes of connected, empty voxels and centre coordinates for every such volume of connected, empty voxels and has the following characteristics:

¹ Certain commercial products are identified in this paper to specify the materials used and procedures employed. In no case does such identification imply endorsement by the National Institute of Standards and Technology, nor does it indicate that the products are necessarily the best available for the purpose.

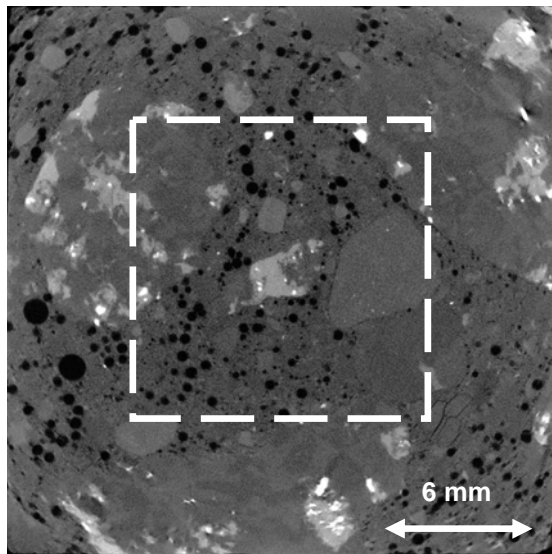


Figure 1: Raw image of the centre xy plane ($z = 551$) of the $1114 \times 1090 \times 1102$ voxel data set. A 500^3 voxel cube is marked with a dotted square. Voxels which are interpreted as empty by CT scanning are coloured black. The shrunken SAP particles will be black due to their low density.

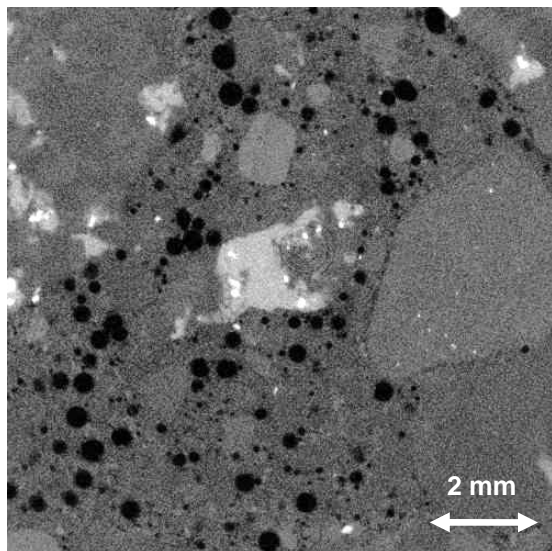


Figure 2: Raw image of the centre xy plane (same cross-section as shown in Figure 1) from the centred 500^3 voxel cube.

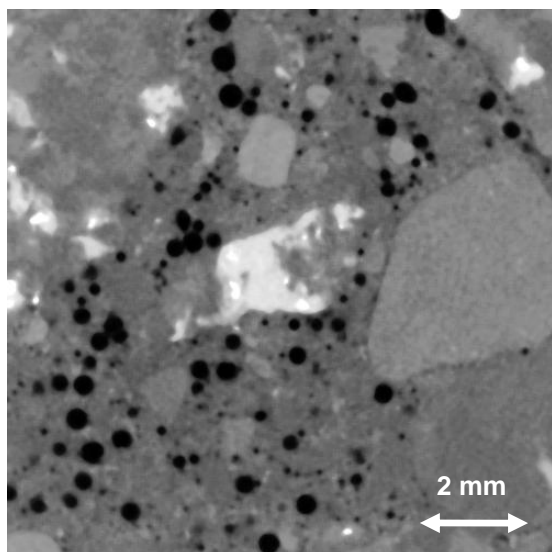


Figure 3: Centre xy plane after application of a $5 \times 5 \times 5$ median filter (same cross-section as shown in Figure 2).

A – Classifies voids as volumes of a minimum of 5 voxels in size, consisting of connected, empty (black) voxels. Approach A interprets a cluster of connected, empty voxels as a single void. A centre xy plane after using approach A is shown in Figure 5. The square marks a cluster of connected, empty voxels which is erroneously interpreted as one void though it clearly is overlapping, individual voids.

B1 – Classifies voids as volumes of a minimum of 5 connected, empty voxels. Approach B1 may separate clusters of empty voxels into individual voids touching each other by use of a so-called watershed algorithm. The term “watershed” is originally used in geology meaning a line separating adjacent draining basins. In this case, “watershed” is used about the plane separating overlapping voids. The watershed algorithm operates by dividing volumes of connected, empty voxels into shells with a thickness of one voxel going from the outside inwards. This creates “bull’s eyes” corresponding to centres of the overlapping, individual voids. Each voxel in the volume of connected empty voxels is attached to the nearest bull’s eye going from the inside outwards. The principle of void separation is shown in Figure 4 to the left. The centre xy plane according to approach B1 is shown in Figure 6. Individual voids are marked with an arbitrary greyscale colour. The square marks the same cluster of empty voxels as in Figure 5. The cluster of connected, empty voxels is interpreted as a number of individual voids touching each other using approach B1. On the other hand, the circle marks an example of a void which is interpreted as two voids even though it is clear that it is only one void.

B2 – Classifies voids as volumes of a minimum of 5 connected empty voxels. Approach B2 is an extension of approach B1. The approach interprets a cluster of connected, empty voxels as one void if there is a maximum of one shell between the bull’s eyes. This means that a cluster of connected, empty voxels is accepted as one void even though it deviates slightly from spherical shape. Figure 4 to the right shows a void with one shell between the two bull’s eyes. This is interpreted as two voids according to approach B1 but only as a single void according to approach B2. The centre xy plane analysed with approach B2 is shown in Figure 7. Individual voids are marked with an arbitrary greyscale colour. The square and the circle mark the same voids as in Figure 6. The circle marked void is interpreted as a single void using approach B2.

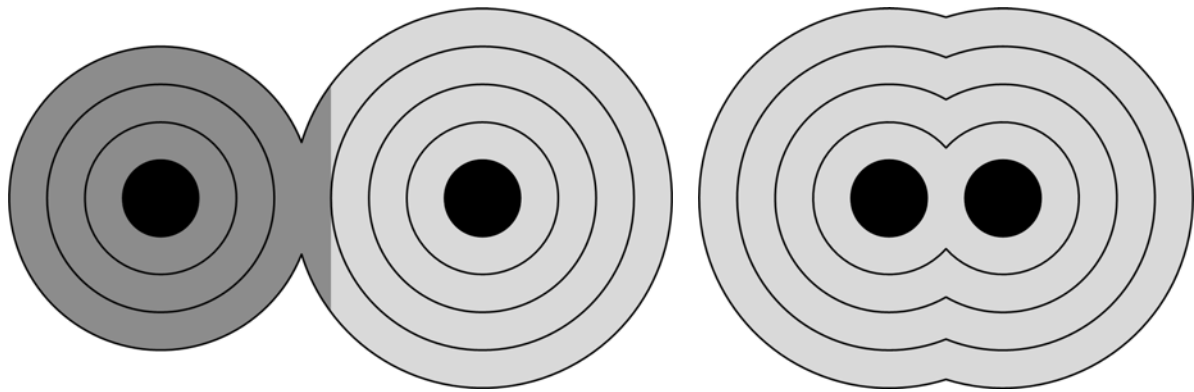


Figure 4: Principle for separating clusters of connected empty voxels. A cluster is divided into one voxel thick shells resulting in “bull’s eyes” marked with black circles. Left: Each voxel is attached to the nearest bull’s eye resulting in a cluster separation into two overlapping, individual voids according to approach B1. Right: The bull’s eyes are only separated by one shell resulting in the cluster being interpreted as a single void according to approach B2.

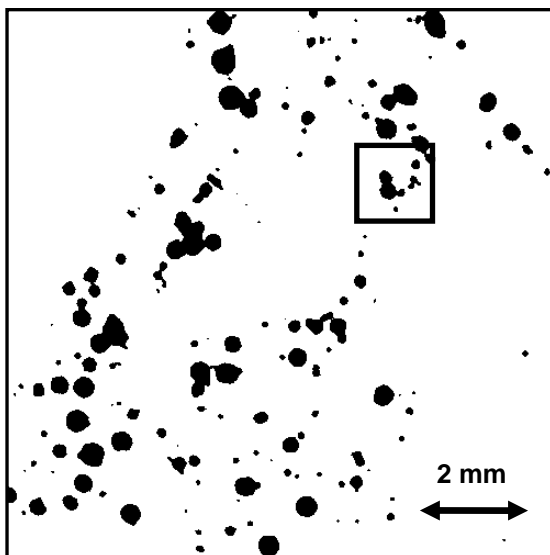


Figure 5: Centre xy plane from the centre 500^3 voxel cube (same as in Figure 2) according to approach A. The square marks a cluster of connected, empty voxels which is interpreted as one void using approach A even though it is clear that it is a number of overlapping, individual voids.

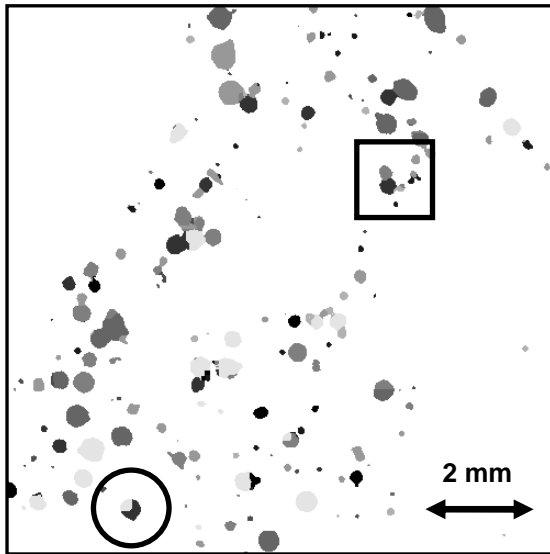


Figure 6: Centre xy plane from the centre 500^3 voxel cube (same as in Figure 2) according to approach B1. Individual voids are marked with an arbitrary greyscale colour. Note that the cluster of connected empty voxels marked with a square are interpreted as a number of overlapping, individual voids contrary to the result using approach A. On the other hand, the circle marks connected, empty voxels which are interpreted as two individual voids using approach B1.

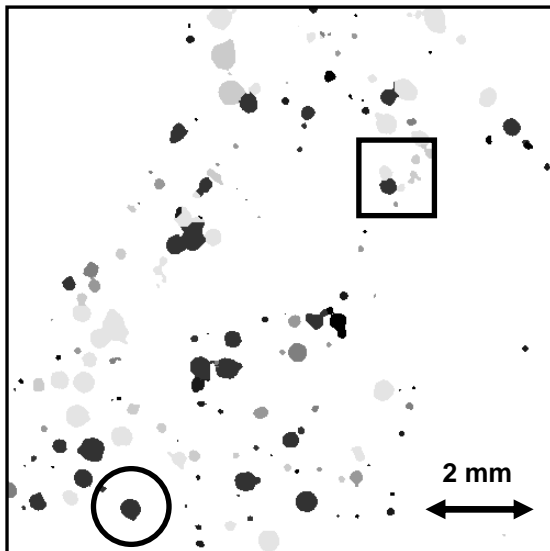


Figure 7: Centre xy plane from the centre 500^3 voxel cube (same as in Figure 2) according to approach B2. Individual voids are marked with an arbitrary greyscale colour. Note that the cluster of connected, empty voxels marked with the square still are interpreted as a number of overlapping, individual voids. Furthermore, the connected, empty voxels marked with a circle are interpreted as one void using approach B2 – compare with the result using approach B1 shown in Figure 6.

4. Results

The calculated air void distributions according to approaches A, B1 and B2 are shown in Figures 8, 9 and 10, respectively. In each case, the void diameters are calculated by assuming the individual void volumes to be spherical.

5. Discussion

The air void distribution in Fig. 8, generated with approach A, has no dominant peak. Conversely, the air void distributions have a dominant peak using approaches B1 and B2, as shown in Figures 9 and 10, respectively. The apparent amount of relatively large voids is reduced using approaches B1 and B2, compared with approach A. This is because approach A interprets any cluster of connected, empty voxels as one void, whereas approaches B1 and B2

allow these to be interpreted as a number of individual voids. The differences in air void distributions between approach A and approaches B1 and B2 indicate the presence of void clusters. Figures 9 and 10 show the air void distributions using approaches B1 and B2. It is seen that the air content of voids smaller than 200 μm is larger using approach B1 than B2. This is believed to be due to too extensive a separation of clusters of connected, empty voxels using approach B1.

The presence of void clusters reduces the homogeneity of the air void system and thereby its usefulness in relation to e.g. freeze-thaw deterioration and internal curing. It would be interesting to analyze if the observed cluster formation is a random, statistical phenomenon or if it is overrepresented. Cluster formation of SAP particles in the fresh concrete may potentially be controlled by chemical modification of the surface properties of the SAP particles. On the other hand, the observed cluster formation may be a result of measuring accuracy or information loss due to the applied filter. This may be a subject for further research. Similarly, it may be relevant to examine if there is a tendency for the SAP particles to be located near aggregate particles.

The position of the dominant peak is at approximately 400 μm according to approach B2 (see Figure 10). The exact position of the peak may be affected by the division of air voids in 50 μm intervals. Using approach B2, the estimated peak position corresponds to an absorption of approximately 11 grams of water per gram dry SAP using approach B2. The estimated absorption, 11 grams of water per gram dry SAP, is in reasonable agreement with previous studies [6,7].

The difference between the measured absorption in previous experiments and the measured absorption based on CT scanning may be due to chemical and physical variation between SAP batches or variations in the concrete environment (such as pore solution concentration). Furthermore, the linear resolution of approximately 20 μm per voxel may not be sufficient for a precise determination of peak position. Also, the threshold value is determined based on a visual assessment. This may imply the risk of an inaccurate assessment that will affect the results using the three approaches. A further investigation should examine if an operator-independent systematic algorithm can be established to generate the binary data set.

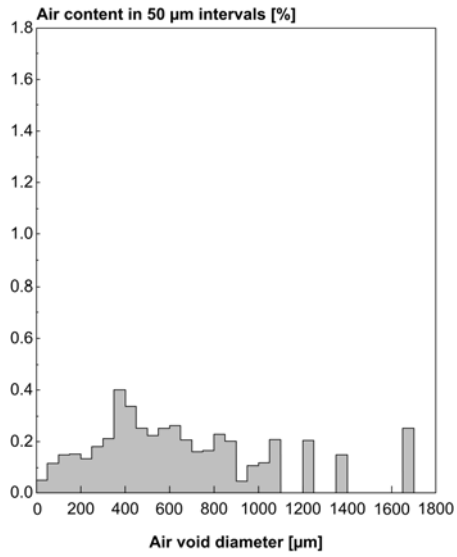


Figure 8: Air contents in 50 μm intervals as a function of air void diameter for approach A.

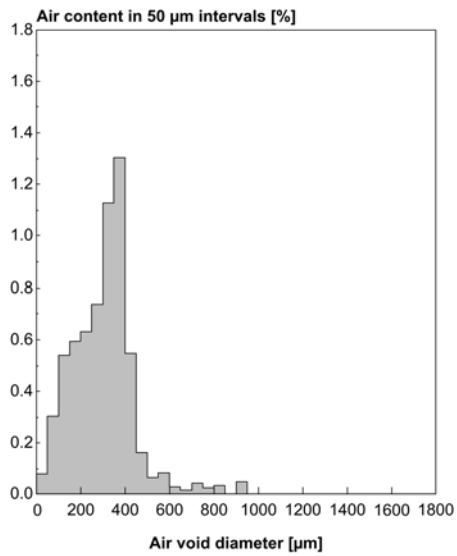


Figure 9: Air contents in 50 μm intervals as a function of air void diameter for approach B1.

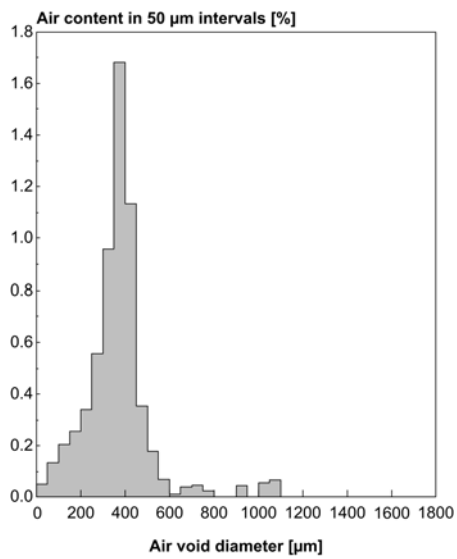


Figure 10: Air contents in 50 μm intervals as a function of air void diameter for approach B2.

The width of the peak is approximately 150 μm using approach B2. The peak width of the swollen SAP particles should be around 30 μm (405 μm to 432 μm), based on a water absorption of 12.5 grams of water per gram dry SAP determined in previous studies [6]. The difference in peak width may be influenced by the voxel size of 20 μm and the subdivision of the air void distribution into 50 μm intervals. However, clarifying the reason for this difference in peak width is a subject for further investigation.

All three approaches disregard connected, empty volumes less than 5 voxels to minimize the effects from noise. This implies that many spherical voids less than 40 μm to 60 μm are eliminated due to the voxel size of 20 μm . Since the diameter of the SAP voids is around 400 μm , it is not critical to quantify voids around 50 μm , but the voxel size of 20 μm may be a limitation, if SAP particles with a smaller diameter are used.

The CT scanned 20 mm x 20 mm x 20 mm specimen may not be representative for bulk concrete as the specimen size is small compared to the maximum aggregate size of 11 mm. Hence, before making comparisons regarding air contents, CT scanning of more specimens from the same concrete mixture should be conducted or the CT measurement should be supplemented with measurement of the composition of the specific specimen.

6. Conclusions

The results show that CT scanning is useful for the determination of the air void distribution of concrete. For SAP voids, it is clearly important that the analysis approach is able to identify individual voids.

The critical points with regards to the analyses methods for SAP voids include filter application and the appropriate determination of a threshold value. Once isolated, individual voids could be further analyzed for supplemental characteristics such as sphericity, etc.

In this study, a relatively narrow size interval of dry SAP particles was added to the concrete. This resulted in a dominant peak in the air void distribution. The peak position corresponds to an absorption of approximately 11 grams of water per gram dry SAP, in agreement with previous measurements.

References

- [1] American Society for Testing and Materials, *ASTM C457 Standard Test Method for Microscopical Determination of Parameters of the Air-Void System in Hardened Concrete*, West Conshohocken, 2009.
- [2] DS/EN 480-11, *Admixtures for concrete, mortar and grout – Test methods – Part 11: Determination of air void characteristics in hardened concrete*, Danish Standard, 2nd edition, Copenhagen, 2005.

- [3] Bentz, D. P., Mizell, S., Satterfield, S., Devaney, J., George, W., Ketcham, P., Graham, J., Porterfield, J., Quenard, D., Vallee, F., Sallee, H., Boller, E., and Baruchel J., *The Visible Cement Data Set*, NIST J. Res. 107(2) (2002) 137-148.
- [4] Promentilla, M. A. B., Sugiyama, T. and Shimura K., *Three-dimensional Image of Cement-based Materials with X-ray Tomographic Microscopy: Visualization and Quantification*, RILEM Proceedings PRO 61 from the 1st International Conference on Microstructure Related Durability of Cementitious Composites, China, 2008, 1357-1366.
- [5] Jensen, O. M. and Hansen, P. F., *Water-entrained cement-based materials I. Principles and theoretical background*, Cement Concrete Res. 31(4) (2001) 647-654.
- [6] Jensen, O. M. and Hansen, P. F., *Water-entrained cement-based materials II. Experimental observations*, Cement Concrete Res. 32(6) (2002) 973-978.
- [7] Laustsen, S. and Madsen, A. M., *Engineered Air-entrainment in Concrete*, Master thesis, Lyngby, Technical University of Denmark, 2007.